Biological Psychiatry: CNNI

Review

Mapping Structure-Function Relationships in the Brain

Abraham Z. Snyder and Adam Q. Bauer

ABSTRACT

Mapping the structural and functional connectivity of the brain is a major focus of systems neuroscience research and will help to identify causally important changes in neural circuitry responsible for behavioral dysfunction. Several methods for examining brain activity in humans have been extended to rodent and monkey models in which molecular and genetic manipulations exist for linking to human disease. In this review, which is part of a special issue focused on bridging brain connectivity information across species and spatiotemporal scales, we address mapping brain activity and neural connectivity in rodents using optogenetics in conjunction with either functional magnetic resonance imaging or optical intrinsic signal imaging. We chose to focus on these techniques because they are capable of reporting spontaneous or evoked hemodynamic activity most closely linked to human neuroimaging studies. We discuss the capabilities and limitations of blood-based imaging methods, usage of optogenetic techniques to map neural systems in rodent models, and other powerful mapping techniques for examining neural connectivity over different spatial and temporal scales. We also discuss implementing strategies for mapping brain connectivity in humans with both basic and clinical applications, and conclude with how cross-species mapping studies can be utilized to influence preclinical imaging studies and clinical practices alike.

Keywords: Effective connectivity, Functional connectivity, Functional neuroimaging, Optogenetics, Structural connectivity, Transcranial magnetic stimulation

https://doi.org/10.1016/j.bpsc.2018.10.005

Representation of function within the brain classically has been understood in terms of focality. For example, expressive language function has been attributed to the left inferior frontal cortex because focal damage to this part of the brain (Broca's area) commonly results in expressive language deficits (1). However, it is increasingly recognized that performance deficits are best understood in terms of functional systems distributed over multiple parts of the brain (2). These functional systems are efficiently studied using resting-state (RS) functional magnetic resonance imaging (fMRI), i.e., fMRI acquired without imposed tasks (3,4). The topographies revealed by such analyses are equivalently known as either RS networks (RSNs) (5) or intrinsic connectivity networks (6). The physiology underlying RSNs remains incompletely understood. While anatomical connectivity [white matter (7–15)] explains many features of functional connectivity (FC) (16), attempts to model whole-brain FC on the basis of connectional anatomy (all known white matter tracts) have been only partially successful (10,17). Thus, anatomical connectivity and FC are related, but not in a simple one-to-one fashion. We shall shortly introduce a third type of connectivity, effective connectivity (EC), which exhibits its own relations to the other connectivity measures. Studying these relations (brain connectomics) and dissecting the complex neural circuitry responsible for brain function (normal or abnormal) has emerged as a major focus of systems neuroscience research (18).

Classically, anatomic connectivity is studied by ex vivo tracing of white matter tracts in brain slices (19). Today, structural connectivity can be noninvasively estimated in vivo using diffusion tensor imaging (8) in combination with computational methods for reconstructing major fiber tracts (7). The basis of RS-FC is that spontaneous fluctuations of blood oxygen level–dependent (BOLD) signals, measured with either fMRI (20) or optical techniques (21), are temporally correlated within RSNs. RSNs commonly are mapped by extracting signals from regions of interest (see below) or computed using spatial independent component analysis (5). Both methods yield reliable and broadly similar results provided that the data are relatively uncorrupted by artifact and acquired over a sufficiently long time (22). The functional significance of RSNs derives from the observation that they topographically correspond to known sensory, motor, and cognitive functional systems (23,24). Compared with task-based measures, RS-FC analyses have provided an efficient method for mapping the whole brain and can be performed in patients incapable of performing tasks (25). Changes in RS-FC have been reported in a variety of neuropsychiatric disorders (26), including Alzheimer's disease (27), depression (28), schizophrenia (29), Parkinson's disease (30), and stroke (31).

BOLD fMRI is the dominant modality for measuring RS-FC in humans and is becoming increasingly more adopted for examining the brain's structure-function relationship in animals

SEE COMMENTARY ON PAGE 506

(9,32,33), including mice (10,34). Importantly, whole-brain functional imaging in mice reveals large-scale functional network architecture corresponding to known murine structural connectivity patterns (10,34). Moreover, basic functional connectional topology is conserved across mice, rats, primates, and humans (35,36). Thus, bridge measurements can be made across animal models to enrich findings in human populations. Given the power of mice to aid in our understanding of human disease, longitudinal mapping techniques that probe brain circuitry more directly could profoundly illuminate pathology-related changes in brain organization.

EC is distinct from, but related to, both anatomical connectivity and FC. EC measures the influence (direct or indirect) that one brain region exerts on another (37). The crucial distinction between RS-FC and EC is that RS-FC characterizes shared spontaneous (ongoing, intrinsic) signals. By definition, pairwise RS-FC is symmetric and uninformative regarding the directionality of propagated signals. Axonal propagation in living animals is physiologically unidirectional (from cell body to axon terminal). However, this directionality cannot be recovered by either histological tract tracing or diffusion tensor imaging–based tractography (38). In contrast, EC reports how activity in an identified part of the brain affects other regions. Thus, measures of EC are not necessarily symmetric. In other words (and neglecting ethical considerations), analyzing RS-FC is analogous to modeling social networks on Facebook by observation of friend relations; studying EC would be analogous to sending provocative material to known Facebook users and analyzing to whom the material spreads.

A frequently used noninvasive mode of studying EC in humans is measuring the influence of task-induced fMRI responses on the BOLD signal in other parts of the brain (39). Transcranial magnetic stimulation (TMS), the other major noninvasive technique for studying EC (40), is discussed at the end of this review. fMRI and TMS aside, the study of EC generally involves invasive techniques, e.g., direct cortical stimulation in patients undergoing surgical evaluation of intractable epilepsy [see Keller *et al.* (41) and Fox *et al.* (42) for recent reviews]. The responses evoked by such stimuli (corticocortical evoked potentials) map out functionally connected regions on the surface of the brain. Corticocortical evoked potential EC exhibits correspondence with anatomical connectivity as determined by diffusion tensor imaging–based tractography (43). Recording electrophysiological responses to injected current has a long history in animal experimentation (11). More recently, the mode of stimulation and/or the means of recording the response have been replaced with more modern techniques such as calcium fluorescence imaging (12) and BOLD fMRI (44). As discussed below, combining optogenetic targeting with wide-field functional neuroimaging represents an even more powerful strategy for examining structure-function relationships in the mammalian brain.

In this review, we examine recently developed methods for EC mapping in animals in combination with optogenetics. We focus on techniques employing hemoglobin as the imaging contrast for linking with human fMRI findings. We use the general term optogenetic EC (Opto-EC) mapping to refer to these strategies for consistency with prior definitions in the literature (37,45). We examine the spatiotemporal capabilities of hemodynamic mapping, as well as other mesoscopic mapping techniques that probe brain activity more directly. Finally, we discuss implementing strategies for mapping EC in the human brain using TMS for both basic and clinical applications, with attention to how cross-species mapping studies can be utilized to influence preclinical imaging studies and clinical practice.

EXAMINING BRAIN CIRCUITS WITH OPTOGENETICS

Optogenetic methods have revolutionized neuroscience by allowing researchers to control genetically defined cell populations through optical stimulation of light-gated, opsin-expressing neurons (46). The most frequently used protein in optogenetics is channelrhodopsin 2 (ChR2), a nonselective cation channel that opens when illuminated with blue light (47), causing the targeted neuron to depolarize. Light-induced hyperpolarization is also possible though illumination of inhibitory opsins (e.g., archaerhodopsin or halorhodopsin) with yellow light (48). Opsin expression can be achieved through a variety of techniques, including viral vector injection for retrograde or anterograde labeling (49), in utero electroporation (50), and transgenic approaches (51). The optogenetic toolbox is constantly evolving (26,52). Red-shifted opsin variants (53) have been developed to allow for deeper tissue penetration or combinatorial excitation or depolarization of different populations of neurons (54). Other developments include the engineering of opsins that exhibit faster kinetics (55) to evoke ultrafast firing frequencies in fast-spiking neurons (56), or "step function" opsins that cause long-term hyper- or hypoexcitability with a single light pulse but revert to prestimulus membrane potentials after a second pulse of light (57). Although the vast majority of optogenetic-based circuit mapping studies have been performed in rodents, use of these techniques has been extended into nonhuman primates (58,59).

Several optogenetic strategies have been implemented to examine neural connectivity over a range of temporal and spatial scales. At the micron scale, optogenetic stimulation in conjunction with multiple whole-cell recording is able to map synaptic connections of individual cells. FC within a microcircuit can be mapped using ChR2-assisted circuit mapping (50). For this method, a single neuron is used as a recording site while multiple regions are stimulated. This method can be used to map local circuitry within a cortical column, for example, in somatosensory barrel cortex (60), or over longer distances spanning several millimeters (61). Maps of specific motor representations can be determined using ChR2-assisted, light-based motor mapping (62). Here, the site of photostimulation is controlled using mirrors, while motor outputs are recorded for quantifying limb (63–65) or whisker (66) movements. This technique can be applied longitudinally, making it an attractive method for tracking cortical reorganization following injury (64). Systems-level connectivity (millimeters to centimeters) can be mapped using optogenetics in conjunction with wide-field mapping of brain activity. Voltage-sensitive dye imaging (67,68), calcium imaging (69,70), and hemodynamic imaging (71–73) have all been successfully applied to measuring Opto-EC in the brain.

Chemogenetic technologies represent another powerful platform for probing genetically targeted, neuroanatomical circuits. The most widely used method, DREADDs (designer

receptors exclusively activated by designer drugs), has been successful in mapping the influence of local circuit activity on global functional network organization across multiple species including mice (74), rats (33), and nonhuman primates (75). Owing to space limitations, chemogenetics are not discussed in detail here. The interested reader is directed to Roth (76) for a review.

HEMODYNAMIC MAPPING OF BRAIN CIRCUITRY

BOLD fMRI and optical intrinsic signal imaging (OISI) have been used extensively to indirectly examine neural activity in the mammalian brain. Understanding how underlying electrophysiological activity, either in single- or multiple-cell populations, relates to the local hemodynamic response is essential for understanding the spatiotemporal capabilities of hemodynamic mapping. See the Supplement for an expanded discussion on using optogenetics to study neurovascular coupling and spatial resolution limits of hemodynamic mapping.

Activity-based mapping of brain circuitry requires examination of stimulus-evoked or spontaneous activity in the brain. We and others have developed methods for mapping local and distant EC using photostimulus-evoked activity with hemodynamic readout in rodents using either Opto-fMRI (72,73,77) or Opto-OISI (71,78–81). For example, in Thy1-ChR2 mice, photostimulation of the left motor cortex (Figure 1A, blue region of interest) results in local hemodynamic responses in

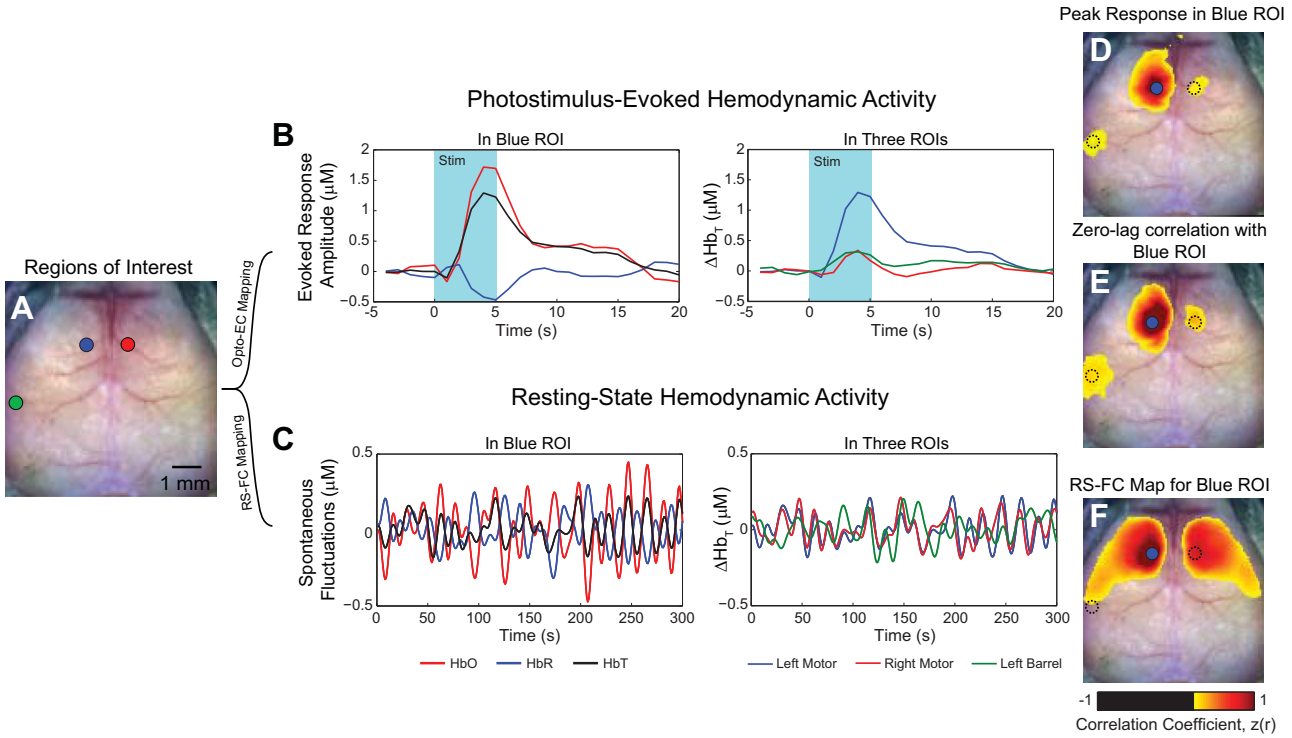

Figure 1. Hemodynamic mapping of brain activity. **(A)** Dorsal view of the exposed, intact mouse skull and regions of interest (ROIs) located in left motor (blue), left barrel (green), and right motor (red) cortices for demonstrating optogenetic effective connectivity (Opto-EC) and resting-state functional connectivity (RS-FC) mapping strategies. **(B)** Left plot: in transgenic thymus cell antigen 1-ChR2 mice, photostimulation of the left motor cortex (473-nm laser light, 0.5 mW, 5-ms pulses delivered at 10 Hz for 5 seconds) results in local hemodynamic responses in oxygenated hemoglobin (HbO) (red), deoxygenated hemoglobin (HbR) (blue), and total hemoglobin (HbT) (black). A single contrast is chosen for further examination of brain connectivity. In this example, we choose HbT because it is most closely related to underlying neural activity and exhibits the highest contrast to noise. Right plot: in the left motor cortex, photostimulus-evoked activity (blue trace) simultaneously evolves with distant hemodynamic activity in the left barrel cortex (green trace) and contralateral right motor cortex (red trace). **(C)** Left plot: in the absence of any overt stimulus, spontaneous fluctuations of all three contrasts can also be measured in the same region. Right plot: co-fluctuations in the same three regions are also observed under RS conditions. Notice, however, that spontaneous activity in the left (blue) and right (red) motor cortices are approximately in phase while fluctuations in the barrel cortex (green) are distinctly less coherent. **(D)** Approximately 5 seconds after photostimulation, a map of peak HbT activity reveals widespread activity in cortical regions surrounding the site of stimulation (blue dot). Additionally, activity in the barrel cortex as well as evoked responses in the homotopic contralateral hemisphere suggest that these satellite regions are functionally connected to the site interrogated. **(E)** Zero-lag correlation between the region stimulated and all other brain regions produces an Opto-EC map (based on thymus cell antigen 1 excitatory stimulation) for the left motor cortex. While topographically similar to the map of peak response in panel **(D)**, the connections with the right motor and left barrel cortices are more pronounced. The time courses in left/right motor and left barrel cortices are all approximately in phase, but of different amplitudes; zero-lag correlation analysis is only sensitive to signal timing and immune to amplitude differences (within noise limits). **(F)** Performing the same zero-lag correlation analysis with spontaneous HbT fluctuations in the left motor cortex produces a RS-FC map for the blue region. Distinct topographical differences exist between the RS-FC map and the Opto-EC map. Unlike the Opto-EC map, the RS-FC map is symmetric at about midline and covers large portions of the motor and lateral somatosensory cortices. RS-FC between the left motor and left barrel cortices is notably absent. Maps in panels **(D)**, **(E)**, and **(F)** are thresholded at a Fisher *z*(*r*) value of 0.3. See Bauer *et al.* (71) for more methodological details.

oxygenated, deoxygenated, and total hemoglobin at stimulated site measured with multispectral OISI (Figure 1B). In the absence of an overt stimulus, intrinsic activity can also be measured (Figure 1C). While each contrast can be used for mapping, oxygenated hemoglobin exhibits the largest signal changes, while total hemoglobin exhibits the highest contrast to noise (71) and is more closely linked to underlying neural activity (82). Single-wavelength OISI takes advantage of the differential absorption profiles of oxygenated and deoxygenated hemoglobin to collect measurements either at wavelengths where oxygenated and deoxygenated hemoglobin absorb light equally [so measurements are sensitive to changes in blood volume (13)] or at wavelengths where one contrast dominates [for collecting measurements sensitive to oxygenation (80,83,84)].

The most straightforward mapping method examines induced activity at a particular time after stimulation. Following photostimulation of the left motor cortex, a map of peak activity (Figure 1D) reveals a response surrounding the site of stimulation. Additionally, activity in the left barrel and right motor cortices suggests that these regions are functionally connected to the site interrogated. We can evaluate these connections using zero-lag correlation between activity in the left motor and all other brain regions to produce a left motor Opto-EC map (Figure 1E). While similar topographically to the map of peak response, connections between the left motor and left barrel are more pronounced. A different picture is observed when examining spontaneous fluctuations (Figure 1C). Performing the same analysis of intrinsic activity shows a symmetric map covering large portions of the motor cortex and lateral somatosensory cortex (Figure 1F). Implementing these strategies for all sites interrogated yields a set of Opto-EC and RS-FC maps over the cortex (Figure 2).

PATTERNS OF OPTO-EC ARE DISTINCT FROM RS-FC MAPS

Several differences between RS-FC and Opto-EC maps are apparent. Stimulation of some regions, e.g., primary and secondary motor regions and the primary barrel cortex, generates distant responses that are not present in the corresponding RS-FC map (Figure 2). Other major differences include the degree to which homotopic regions share coordinated activity. Bilaterally symmetric RS-FC is very well documented in multiple species on the basis of fMRI and optical techniques (9,13,14,20,21,85). A profound lack of homotopic EC is observed in the barrel, visual, and posterior parietal regions (Figure 2). These Opto-EC versus RS-FC differences may provide insights into the nature of spontaneous activity. Synchronous activity in homotopic cortical regions, as reflected in RS-FC maps, may reflect monosynaptic, transcallosal connections or coordination by subcortical structures. RS-FC in the visual cortex of monkeys most likely involves polysynaptic pathways (9), and indirect corticocortical structural connectivity predicts interhemispheric RS-FC between human visual cortices (86). Additionally, the thalamus can regulate cortical excitability (87) and may do so selectively so that homotopic regions are excitable at the same time (15,88,89).

OPTO-EC MATCHES AXONAL PROJECTION CONNECTIVITY MORE CLOSELY THAN RS-FC

Given the differences between Opto-EC and RS-FC patterns, it is reasonable to hypothesize that one method reflects more directly underlying anatomical connectivity. We recently compared Opto-EC to patterns of axonal projection connectivity (APC) (71) collected from the Allen Mouse Brain

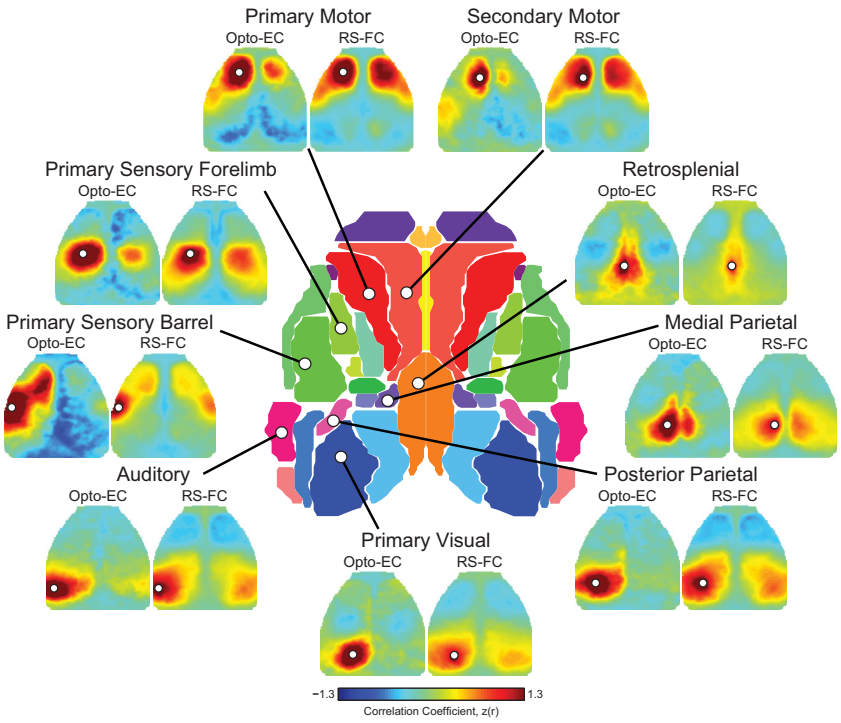

Figure 2. Cortical patterns of optogenetic effective connectivity (Opto-EC) and resting-state functional connectivity (RS-FC). Thymus cell antigen 1–based, Opto-EC maps in 5 mice calculated by zero-lag correlation of the evoked time course at the stimulated site and activity over the rest of the brain during a 25-second epoch as well as RS-FC maps in 8 mice calculated by zero-lag correlation of spontaneous time courses at the coordinates of stimulated sites and the rest of the brain (20–30 min/mouse) during a separate imaging session. All connectivity images were created using total hemoglobin as contrast. While the maps share features, the RS-FC maps are both qualitatively and quantitatively different from their Opto-EC counterparts. For example, the secondary motor cortex demonstrates ipsilateral EC with the barrel cortex that is not present in the RS-FC map, and RS-FC maps are largely bilaterally symmetric. Further details can be found in Bauer *et al.* (71). Modified with permission from Bauer *et al.* (71).

Connectivity Atlas (90). For most sites evaluated, the similarities between the APC images and the Opto-EC maps were significantly higher compared with the RS-FC and APC maps (Figure 3A). The highest overlap between Opto-EC and APC occurred in sensorimotor cortices (where the RS-FC patterns overlapped least). Interestingly, hemodynamic measures of Opto-EC within sensorimotor cortices appear to reflect the known input-output organization of these regions (motor and barrel regions in Figures 2 and 3A). In rodents, whisker-based tactile sensation and sensorimotor integration are mediated by a connection loop between somatosensory barrel and motor cortices (91). We observe appreciable connection strength asymmetry between the primary motor cortex (M1) and the lateral barrel region of the somatosensory cortex, agreeing with previous studies reporting directionality within this system using invasive anatomical tracing (91) and other local (50,61) and global (63,68) in vivo ChR2-based methods measuring neural activity more directly. The similarity between Opto-EC and APC suggests that Opto-EC patterns tend to reflect pairwise connectivity between neurons, much like electrical stimulation of the cortex (92), whereas RS-FC appears to largely reflect polysynaptic pathways.

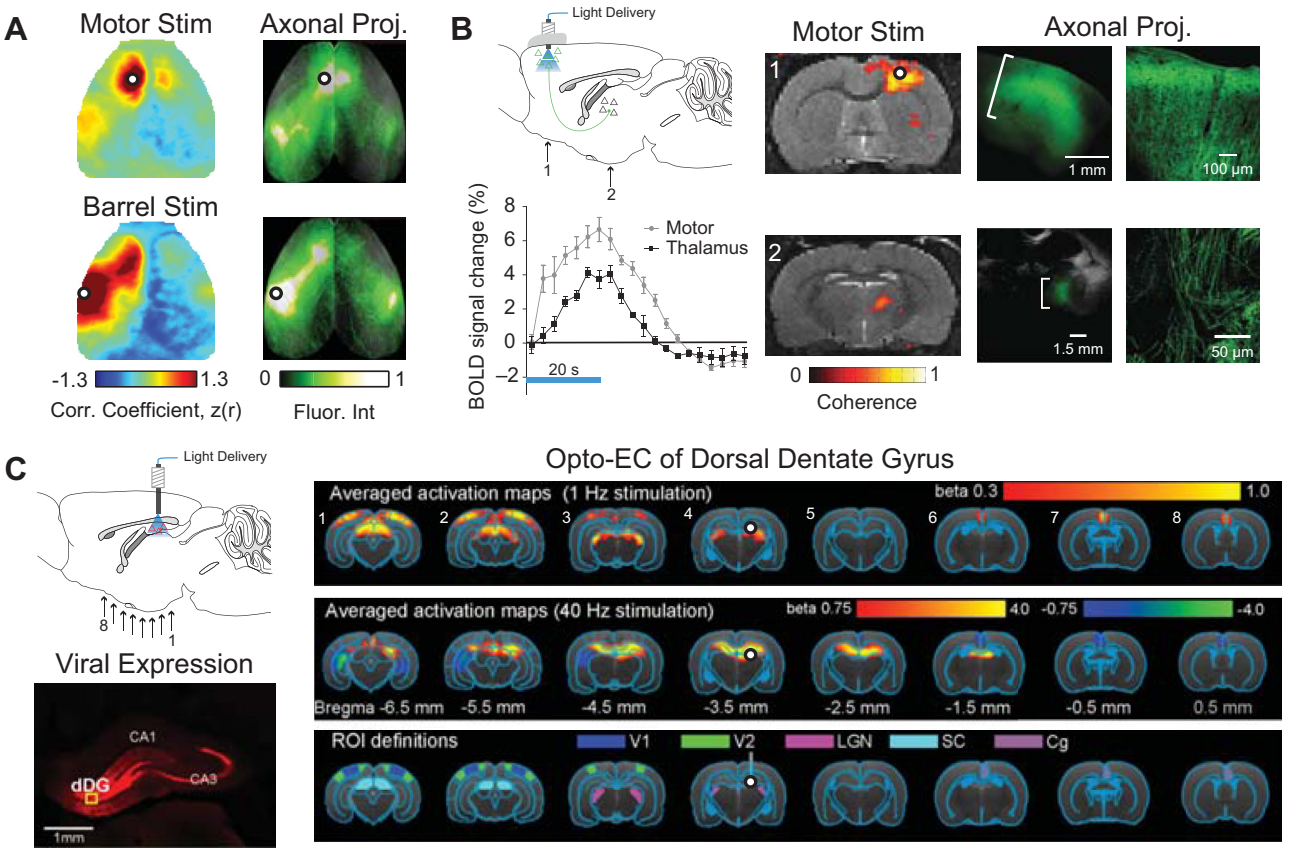

Figure 3. Global optogenetic effective connectivity (Opto-EC) mapping to probe brain anatomy and function. **(A)** Maps of thymus cell antigen 1–based Opto-EC and resting-state functional connectivity are compared with axonal projection connectivity (APC) images from the Allen Mouse Brain Connectivity Atlas. APC images were acquired using the source search feature within the Mouse Connectivity Data Portal and projected onto the cortical surface using the cortical map signal viewer, co-registered to optical intrinsic signal imaging data and normalized by maximum fluorescence intensity. Generally, thymus cell antigen 1–based, Opto-EC maps report monosynaptic cortical connectivity structure but can be collected in awake, behaving animals. See Bauer *et al.* (71) for more details. **(B)** Nonlocal mapping of cells defined by location and genetic identity. Top left: viral injection (adeno-associated virus 5–calcium/calmodulin-dependent protein kinase type II alpha chain::channelrhodopsin 2–enhanced yellow fluorescent protein) and optical stimulation in the primary motor cortex results in local (Motor Stim) (image 1) and distant (thalamus) (image 2) blood oxygen level–dependent (BOLD) responses. Fluorescence/bright-field images show channelrhodopsin 2–enhanced yellow fluorescent protein expression in the motor and thalamic regions while confocal images show that expression is limited to axons. Modified with permission from Lee *et al.* (73). **(C)** Hippocampal–cortical pathways contribute to global resting-state functional connectivity in the rodent. Viral injection of channelrhodopsin 2::calcium/calmodulin-dependent protein kinase type II alpha chain in dorsal dentate gyrus (dDG) excitatory neurons. Arrows below the brain image indicate approximate locations of Opto-EC activation maps numbered one (posterior) through eight (anterior). Histology image shows mCherry fluorescence from viral expression in the dorsal hippocampus. Brain-wide activation maps of visually related regions during low-frequency optogenetic stimulation of dDG excitatory neurons. Top row: averaged activation maps from 1-Hz photostimuli delivered to dDG show robust positive BOLD responses detected in bilateral primary visual cortex (V1), secondary visual cortex (V2), lateral geniculate nucleus (LGN), and superior colliculus (SC), as well as the cingulate cortex (Cg). Middle row: high-frequency optogenetic stimulation (40 Hz) of dDG excitatory neurons in the dorsal hippocampus does not evoke brain-wide cortical and subcortical activation in V1, V2, LGN, and SC. Bottom row: regions of interest (ROIs). Modified with permission from Chan *et al.* (89). In all images, the white dot with black outline indicates the stimulation site. Corr., correlation; Int, intensity; Proj., projections.

GLOBAL OPTO-EC MAPPING TO PROBE BRAIN ANATOMY AND FUNCTION

The recent integration of optogenetics with fMRI and OISI has allowed for examining the effects of precise optogenetic manipulations on global brain activity. The first Opto-fMRI study delivered light to the motor cortex as well as thalamic targets to reveal BOLD responses resulting from local excitatory neural activity (73) (Figure 3B). Reciprocal stimulation of the anterior thalamic nucleus resulted in bilateral motor responses, whereas stimulation of the posterior thalamic nucleus resulted in ipsilateral somatosensory responses. These findings demonstrate not only different cortical projections of thalamic nuclei, in line with neural tracing studies, but also a thalamic role in shaping coherent spontaneous activity across hemispheres (15).

Changes in infraslow (<0.1 Hz) spontaneous activity (e.g., as reflected in patterns of RS-FC) facilitate and modulate a diverse set of motor, sensory, and cognitive processes. However, the neural basis of RS-FC remains unknown. Most studies have only correlated measures of neural activity with hemodynamics instead of directly probing the effects of modulated, region-specific electrical activity on global RS-FC. With its dense reciprocal APC to and from the cortex, the hippocampus is believed to mediate numerous cognitive functions and sensory processing (93). Further, cortical slow oscillations (1 Hz), which are phase-locked with cellular activity in the dentate gyrus (94), resemble the spatiotemporal characteristics of infraslow activity in RSNs. Thus, low-frequency activity in hippocampal–cortical pathways could contribute to global RS-FC to integrate sensory information. Chan *et al.* (89) examined large-scale effects of spatiotemporal-specific propagation of downstream hippocampal activity on global RS-FC. In that study, stimulation of excitatory neurons in the dorsal dentate gyrus at low frequency (1 Hz), but not at high frequency (40 Hz), evoked robust cortical and subcortical brain-wide responses (Figure 3C). Low-frequency stimulation enhanced interhemispheric hippocampal and cortical RS-FC. Local field potential recordings revealed an increase in slow oscillations in the hippocampus and visual cortex, interhemispheric visual RS-FC, and hippocampal–cortical RS-FC. Together, these results highlight the role of low-frequency activity propagating along the hippocampal–cortical pathway, and its contribution to interhemispheric cortical RS-FC.

Opto-EC mapping can also identify large-scale brain networks corresponding to specific behavioral and electrophysiological markers. For example, the thalamus plays a crucial role in coordinating brain signaling responsible for cognition and normal waking behavior (95). The central thalamus and intralaminar nuclei are postulated to regulate arousal, attention, and goal-oriented behavior (96). Using Opto-fMRI in conjunction with electrophysiology, Liu *et al.* (97) examined the thalamic-driven global brain networks responsible for switching across brain states with activity corresponding to electrophysiological metrics of arousal (e.g., spindle-like oscillations). In a separate study, stimulation of excitatory cells in intermediate hippocampus caused widespread BOLD signaling at high frequencies and predicted seizure-like afterdischarges in electroencephalographic recordings and behavioral output (98).

EC MAPPING IN HUMANS

Noninvasive strategies for mapping brain connectivity in the human brain have primarily employed TMS, which offers a less painful alternative to current injection through the scalp (99). The basic principle underlying TMS is that a rapidly switched current though a coil placed over the scalp induces an electric potential around the coil that stimulates the brain. Repetitive TMS (rTMS) refers to pulse train stimulation at frequencies in the range of 1 to 50 Hz. Pulse trains of duration on the order of few seconds often are delivered over minutes with the objective of inducting temporary changes in cortical excitability. Whether rTMS is inhibitory or excitatory has been thought to depend on pulse frequency (<1 Hz: inhibitory; >5 Hz: excitatory) (100). However, the sign of observed effects does not always follow this rule (40,101). Theta-burst TMS (brief pulse trains [3 pulses at 50 Hz], rhythmically delivered at theta frequencies [5 Hz]) over tens of minutes is frequently used to induce plasticity (102).

Basic physiological investigations in animals have established that several seconds of rTMS initially increases cerebral blood flow (CBF) immediately under the coil; the initial response lasts on the order of a minute, after which blood flow becomes depressed (103). Similar physiologic "activation" responses have been observed with [^{14}C]-deoxyglucose autoradiography (104) and measurement of regional CBF using [^{15}O]H_2O positron emission tomography (105). In humans, increases in CBF have been observed using arterial spin labeling MRI (106) and near-infrared spectroscopy (107). Importantly, these physiological responses do not reflect enhanced neural function. Single-unit discharge under the coil might variably increase or decrease following rTMS (108), while neural responses to natural stimuli generally are disrupted (103). This effect commonly is referred to as a "virtual lesion" (109). For example, occipital rTMS disrupts RS-FC within the visual system and degrades performance on a visual discrimination task (110). A particularly informative example of the virtual lesion effect was observed in an experiment in which 10-Hz occipital rTMS impaired Braille reading in lifelong blind individuals, thereby demonstrating that a part of the brain normally used for vision had been reconfigured to analyze haptic (tactile) information (111). A recent meta-analysis of 29 studies confirmed that continuous theta-burst rTMS reliably impairs executive function (112). However, exceptions to this general rule exist. In normal volunteers, 20-Hz parietal rTMS (daily 2-second bursts every 30 seconds × 20 minutes × 5 days) increased FC within the hippocampal-parietal memory system and significantly improved associative memory performance (113).

To study EC, TMS is combined with additional techniques including electroencephalography (114), magnetoencephalography (115), positron emission tomography (116), near-infrared spectroscopy (117), or fMRI (118). The variety of such multimodal TMS experiments is thoroughly covered in recent reviews (40,119). Combining TMS with electroencephalography arguably is methodologically most similar to the above-reviewed Opto-EC studies in rodents. Thus, single-pulse TMS delivered to the left motor cortex reliably evokes electrophysiological responses that evolve over ~400 ms to involve functionally related parts of the brain (120). Most

experiments combining fMRI with TMS stimulate with pulse trains (i.e., rTMS) and measure BOLD responses both under the coil and in functionally related parts of the brain remote from the stimulated site (121,122). The response may depend on whether the remote region is engaged by a concurrently administered behavioral task. For example, 10-Hz right parietal rTMS (delivered alone) depresses CBF in the left primary sensory cortex; however, in the presence of right median nerve shocks, CBF in the left somatosensory cortex is enhanced. Moreover, 10-Hz right parietal rTMS enhances detection of near-threshold right median nerve stimuli (123). Similar state-dependent modulations of EC between the dorsal premotor cortex and motor cortex have been demonstrated with motor tasks (124).

A wide variety of neurologic and psychiatric disorders have implemented TMS therapy (125). The rational basis for the therapeutic effect is specific to condition. Unilateral stroke might destroy the part of the brain controlling motor function on the opposite side of the body. It follows that weakness contralateral to the stroke is attributable to loss of function. However, interference from the intact hemisphere, which often is overactive, also is a factor. Thus, inhibitory (1 Hz) TMS over the intact hemisphere as well as excitatory (10 Hz) stimulation over the lesioned hemisphere may improve motor function of the paretic hand (126). In Parkinson's disease, the physiological abnormality responsible for rigidity and bradykinesia (inability to initiate action) is persistent, abnormally hypersynchronous beta (15–30 Hz) activity throughout the motor system (cortex, basal ganglia, thalamus). High-frequency stimulation of the subthalamic nucleus via implanted electrodes often restores mobility by disrupting the pathological hypersynchrony (127). High-frequency rTMS of the motor cortex offers a noninvasive (but less permanent) alternative that could work via the same mechanism (128).

FROM MAN TO MOUSE TO MAN: ITERATING BETWEEN PRECLINICAL AND CLINICAL FINDINGS

Depression is the condition most often treated by rTMS. Converging neuroanatomical and postmortem histological evidence points to the ventromedial prefrontal cortex (VMPFC) as a specific locus of dysfunction in depression (129). rTMS offers a noninvasive alternative to deep brain stimulation, but the challenge is that VMPFC is a deep structure not directly accessible to TMS. However, experimental evidence indicates that rTMS can be optimized by targeting a specific region in the dorsolateral PFC known to be maximally anticorrelated with the VMPFC in normal individuals (130). This result represents a case in which RS-FC mapping in normal subjects has informed the clinical therapy of depression. Clinical efficacy may be further improved by targeting the specific dorsolateral PFC region maximally anticorrelated with VMPFC individually identified in each patient using information gleaned from RS-FC mapping (131).

Further dissection of PFC circuitry via EC mapping in animal models could also help to improve the specificity of targeted therapy. Depression is linked to several neural pathways and to distinct neuromodulatory systems and receptors (52). In animal models of depression, the medial PFC is the most typically examined and has been dissected anatomically and functionally using optogenetics. For example, selective activation or suppression of VMPFC circuits in rodents has established the causal relationship between medial PFC connectivity and depression-like behaviors (132,133). Mesolimbic dopamine circuitry is also widely studied in models of depression (134). A key component of this circuitry is dopamine neurons in the ventral tegmental area (VTA) that project to the limbic regions, such as the nucleus accumbens, amygdala, and PFC (135). This mesolimbic system is thought to be functionally distinct from dopamine-innervated basal ganglia regions. However, Lohani *et al.* (136) demonstrate that phasic stimulation of VTA dopamine neurons increased BOLD signaling in known VTA-innervated regions, but also in regions that receive little or no VTA dopaminergic input (thalamus, hippocampus, and dorsal striatum). Thus, Opto-EC mapping is capable of identifying novel circuits within RSNs for probing questions about causal changes in circuit communication responsible for behavioral dysfunction. Compared with other diseases, the myriad symptoms that define clinical depression cannot all be accurately modeled in animals. One strategy for linking clinical

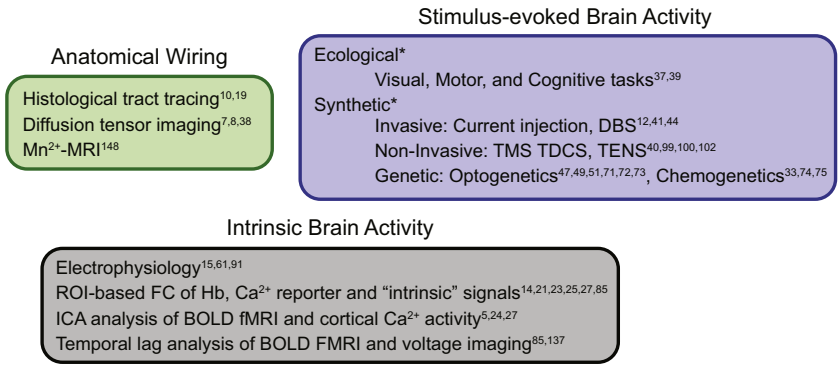

Figure 4. Tools for mapping brain connectomics. Mapping anatomical, or white matter, connections of the brain can be performed with ex vivo histological tract tracing (10,19) or in vivo using diffusion tensor imaging (7,8,38) or manganese-enhanced magnetic resonance imaging (Mn^{2+}-MRI) (148). Mapping the functional organization of the brain can be performed in vivo by invoking ecological (physiologically normal) stimuli as functional localizers (37,39), or via synthetic (nonphysiological) stimuli via invasive (12,41,44), noninvasive (40,99,100,102), or genetics-based (33,47,49,51,71–75) strategies. In the absence of any overt task, ongoing spontaneous or intrinsic brain activity can be evaluated through electrophysiology (15,61,91), region of interest (ROI)–based (14,21,23,25,27,85), or independent component analysis (ICA)–based (5,24,27) analyses, as well as through evaluating the relative timing differences in regional activity propagation (temporal lag analysis) (85,137). BOLD, blood oxygen level–dependent; Ca^{2+}, calcium; DBS, deep brain stimulation; FC, functional connectivity; fMRI, functional magnetic resonance imaging; Hb, hemoglobin; TDCS, transcranial direct current stimulation; TENS, transcutaneous electrical nerve stimulation; TMS, transcranial magnetic stimulation.

findings in patients with experimental work (and vice versa) would be to focus on human behavioral symptoms having measurable correlates in animal models.

CONCLUSIONS

We have reviewed several related but distinct forms of mapping brain connectivity: anatomical connectivity (white matter tracts), EC (how activity in one part of brain affects function elsewhere), and FC (correlated infraslow spontaneous activity) (Figure 4). Owing to space limitations, we have omitted discussion of many important topics, for example, that infraslow spontaneous activity, as imaged with hemoglobin-dependent signals, propagates over centimeter-scale distances at velocities far slower than axonal propagation of action potentials (137). The physiology underlying this phenomenon currently is not understood.

Much of the presently reviewed findings were obtained in mice but very likely apply to humans, as basic principles of brain connectomics are conserved across a wide range of species (36). We have focused on recently developed methods capable of specifically stimulating excitatory (68,71,72,81) or inhibitory (73,78) neurons. New technologies for examining responses include calcium signaling within neurons (137–140) or astrocytes (141). Advances in genetically encoded, fluorescent protein voltage indicators continues to progress (142,143); this technology may eliminate some of the problems associated with voltage-sensitive dye signaling (indiscriminate labeling, cytotoxicity) and could allow for wide-field, systems-level, all-optical electrophysiology (144,145). These methods, perhaps in combination with red-shifted opsins, will undoubtedly reveal temporal processes and other aspects of neural interactions important for sustaining normal brain function.

We concluded this review with brief overview of human rTMS with an emphasis on treatment of depression. As discussed above, multiple lines of evidence derived from animal experimentation support rTMS as a treatment for depression. However, notwithstanding its widespread use, the efficacy of rTMS as a treatment for depression has not been established (146). A recent meta-analysis of 61 published studies suggests that a significant fraction of positive clinical responses is attributable the placebo effect (147). Thus, there remains a gap between the rich body of accumulated connectomics knowledge and practical clinical application. This is not cause for discouragement, as basic science eventually leads to practical benefits.

ACKNOWLEDGMENTS AND DISCLOSURES

This work was supported by National Institutes of Health Grant Nos. R01NS102870 (to AQB), K25NS083754 (to AQB), P01NS080675 (to AZS), and P30NS098577 (to AZS).

The authors report no biomedical financial interests or potential conflicts of interest.

ARTICLE INFORMATION

From the Department of Radiology, Washington University School of Medicine, St. Louis, Missouri.

Address correspondence to Adam Bauer, Ph.D., Washington University School of Medicine, Couch Research Building, 4515 McKinley Ave, St. Louis, MO 63110; E-mail: aqbauer@wustl.edu.

Received Aug 13, 2018; revised and accepted Oct 17, 2018.

Supplementary material cited in this article is available online at https://doi.org/10.1016/j.bpsc.2018.10.005.

REFERENCES

1. Mohr JP, Pessin MS, Finkelstein S, Funkenstein HH, Duncan GW, Davis KR (1978): Broca aphasia: Pathologic and clinical. Neurology 28:311–324.
2. Siegel JS, Ramsey LE, Snyder AZ, Metcalf NV, Chacko RV, Weinberger K, *et al.* (2016): Disruptions of network connectivity predict impairment in multiple behavioral domains after stroke. Proc Natl Acad Sci U S A 113:E4367–E4376.
3. Biswal B, Yetkin FZ, Haughton VM, Hyde JS (1995): Functional connectivity in the motor cortex of resting human brain using echo-planar MRI. Magn Reson Med 34:537–541.
4. Raichle ME (2015): The restless brain: How intrinsic activity organizes brain function. Philos Trans R Soc Lond B Biol Sci 370: 20140172.
5. Beckmann CF, DeLuca M, Devlin JT, Smith SM (2005): Investigations into resting-state connectivity using independent component analysis. Philos Trans R Soc Lond B Biol Sci 360:1001–1013.
6. Seeley WW, Menon V, Schatzberg AF, Keller J, Glover GH, Kenna H, *et al.* (2007): Dissociable intrinsic connectivity networks for salience processing and executive control. J Neurosci 27:2349–2356.
7. Behrens TEJ, Berg HJ, Jbabdi S, Rushworth MFS, Woolrich MW (2007): Probabilistic diffusion tractography with multiple fibre orientations: What can we gain? Neuroimage 34:144–155.
8. Le Bihan D (2003): Looking into the functional architecture of the brain with diffusion MRI. Nat Rev Neurosci 4:469–480.
9. Vincent JL, Patel GH, Fox MD, Snyder AZ, Baker JT, Van Essen DC, *et al.* (2007): Intrinsic functional architecture in the anaesthetized monkey brain. Nature 447:83–86.
10. Grandjean J, Zerbi V, Balsters JH, Wenderoth N, Rudin M (2017): Structural basis of large-scale functional connectivity in the mouse. J Neurosci 37:8092–8101.
11. Asanuma H, Stoney SD Jr, Abzug C (1968): Relationship between afferent input and motor outflow in cat motorsensory cortex. J Neurophysiol 31:670–681.
12. Histed MH, Bonin V, Reid RC (2009): Direct activation of sparse, distributed populations of cortical neurons by electrical microstimulation. Neuron 63:508–522.
13. Kura S, Xie H, Fu B, Ayata C, Boas DA, Sakadzic S (2018): Intrinsic optical signal imaging of the blood volume changes is sufficient for mapping the resting state functional connectivity in the rodent cortex. J Neural Eng 15:035003.
14. White BR, Bauer AQ, Snyder AZ, Schlaggar BL, Lee JM, Culver JP (2011): Imaging of functional connectivity in the mouse brain. PLoS One 6:e16322.
15. Xiao D, Vanni MP, Mitelut CC, Chan AW, LeDue JM, Xie Y, *et al.* (2017): Mapping cortical mesoscopic networks of single spiking cortical or sub-cortical neurons. eLife 6:e19976.
16. Behrens TE, Sporns O (2012): Human connectomics. Curr Opin Neurobiol 22:144–153.
17. Honey CJ, Thivierge JP, Sporns O (2010): Can structure predict function in the human brain? Neuroimage 52:766–776.
18. Fornito A, Zalesky A, Breakspear M (2015): The connectomics of brain disorders. Nat Rev Neurosci 16:159–172.
19. Jones EG (1999): Making brain connections: Neuroanatomy and the work of TPS Powell, 1923-1996. Annu Rev Neurosci 22:49–103.
20. Shehzad Z, Kelly AM, Reiss PT, Gee DG, Gotimer K, Uddin LQ, *et al.* (2009): The resting brain: Unconstrained yet reliable. Cereb Cortex 19:2209–2229.
21. Eggebrecht AT, Ferradal SL, Robichaux-Viehoever A, Hassanpour MS, Dehghani H, Snyder AZ, *et al.* (2014): Mapping distributed brain function and networks with diffuse optical tomography. Nat Photonics 8:448–454.
22. Laumann TO, Gordon EM, Adeyemo B, Snyder AZ, Joo SJ, Chen MY, *et al.* (2015): Functional system and areal organization of a highly sampled individual human brain. Neuron 87:657–670.

23. Power JD, Cohen AL, Nelson SM, Wig GS, Barnes KA, Church JA, *et al.* (2011): Functional network organization of the human brain. Neuron 72:665–678.
24. Smith SM, Fox PT, Miller KL, Glahn DC, Fox PM, Mackay CE, *et al.* (2009): Correspondence of the brain's functional architecture during activation and rest. Proc Natl Acad Sci U S A 106:13040–13045.
25. Hacker CD, Laumann TO, Szrama NP, Baldassarre A, Snyder AZ, Leuthardt EC, *et al.* (2013): Resting state network estimation in individual subjects. Neuroimage 82:616–633.
26. Gradinaru V, Zhang F, Ramakrishnan C, Mattis J, Prakash R, Diester I, *et al.* (2010): Molecular and cellular approaches for diversifying and extending optogenetics. Cell 141:154–165.
27. Buckner RL, Sepulcre J, Talukdar T, Krienen FM, Liu H, Hedden T, *et al.* (2009): Cortical hubs revealed by intrinsic functional connectivity: Mapping, assessment of stability, and relation to Alzheimer's disease. J Neurosci 29:1860–1873.
28. Alexopoulos GS, Hoptman MJ, Kanellopoulos D, Murphy CF, Lim KO, Gunning FM (2012): Functional connectivity in the cognitive control network and the default mode network in late-life depression. J Affect Disord 139:56–65.
29. Fox MD, Snyder AZ, McAvoy MP, Barch DM, Raichle ME (2005): The BOLD onset transient: Identification of novel functional differences in schizophrenia. Neuroimage 25:771–782.
30. Gratton C, Koller JM, Shannon W, Greene DJ, Maiti B, Snyder AZ, *et al.* (2019): Emergent functional network effects in Parkinson disease. Cereb Cortex 29:2509–2523.
31. Carter AR, Patel KR, Astafiev SV, Snyder AZ, Rengachary J, Strube MJ, *et al.* (2012): Upstream dysfunction of somatomotor functional connectivity after corticospinal damage in stroke. Neurorehabil Neural Repair 26:7–19.
32. Otte WM, van der Marel K, van Meer MP, van Rijen PC, Gosselaar PH, Braun KP, *et al.* (2015): Altered contralateral sensorimotor system organization after experimental hemispherectomy: A structural and functional connectivity study. J Cereb Blood Flow Metab 35:1358–1367.
33. Roelofs TJM, Verharen JPH, van Tilborg GAF, Boekhoudt L, van der Toorn A, de Jong JW, *et al.* (2017): A novel approach to map induced activation of neuronal networks using chemogenetics and functional neuroimaging in rats: A proof-of-concept study on the mesocorticolimbic system. Neuroimage 156:109–118.
34. Stafford JM, Jarrett BR, Miranda-Dominguez O, Mills BD, Cain N, Mihalas S, *et al.* (2014): Large-scale topology and the default mode network in the mouse connectome. Proc Natl Acad Sci U S A 111:18745–18750.
35. van den Heuvel MP, Bullmore ET, Sporns O (2016): Comparative connectomics. Trends Cogn Sci 20:345–361.
36. Betzel RF, Bassett DS (2018): Specificity and robustness of long-distance connections in weighted, interareal connectomes. Proc Natl Acad Sci U S A 115:E4880–E4889.
37. Friston KJ, Frith CD, Frackowiak RSJ (1993): Time-dependent changes in effective connectivity measured with PET. Hum Brain Mapp 1:69–79.
38. Mukherjee P, Berman JI, Chung SW, Hess CP, Henry RG (2008): Diffusion tensor MR imaging and fiber tractography: Theoretic underpinnings. AJNR Am J Neuroradiol 29:632–641.
39. Friston KJ (2011): Functional and effective connectivity: A review. Brain Connect 1:13–36.
40. Hallett M, Di Iorio R, Rossini PM, Park JE, Chen R, Celnik P, *et al.* (2017): Contribution of transcranial magnetic stimulation to assessment of brain connectivity and networks. Clin Neurophysiol 128:2125–2139.
41. Keller CJ, Honey CJ, Megevand P, Entz L, Ulbert I, Mehta AD (2014): Mapping human brain networks with cortico-cortical evoked potentials. Philos Trans R Soc Lond B Biol Sci 369:20130528.
42. Fox KCR, Foster BL, Kucyi A, Daitch AL, Parvizi J (2018): Intracranial electrophysiology of the human default network. Trends Cogn Sci 22:307–324.
43. Donos C, Maliia MD, Mindruta I, Popa I, Ene M, Balanescu B, *et al.* (2016): A connectomics approach combining structural and effective connectivity assessed by intracranial electrical stimulation. Neuroimage 132:344–358.
44. Tolias AS, Sultan F, Augath M, Oeltermann A, Tehovnik EJ, Schiller PH, *et al.* (2005): Mapping cortical activity elicited with electrical microstimulation using FMRI in the macaque. Neuron 48:901–911.
45. Ryali S, Shih YI, Chen T, Kochalka J, Albaugh D, Fang Z, *et al.* (2016): Combining optogenetic stimulation and fMRI to validate a multivariate dynamical systems model for estimating causal brain interactions. Neuroimage 132:398–405.
46. Boyden ES, Zhang F, Bamberg E, Nagel G, Deisseroth K (2005): Millisecond-timescale, genetically targeted optical control of neural activity. Nat Neurosci 8:1263–1268.
47. Nagel G, Szellas T, Huhn W, Kateriya S, Adeishvili N, Berthold P, *et al.* (2003): Channelrhodopsin-2, a directly light-gated cation-selective membrane channel. Proc Natl Acad Sci U S A 100:13940–13945.
48. Chow BY, Han X, Boyden ES (2012): Chapter 3 - Genetically encoded molecular tools for light-driven silencing of targeted neurons. In: Knöpfel T, Boyden ES, editors. Progress in Brain Research. New York: Elsevier, 49–61.
49. Zhang F, Wang LP, Boyden ES, Deisseroth K (2006): Channelrhodopsin-2 and optical control of excitable cells. Nat Methods 3: 785–792.
50. Petreanu L, Huber D, Sobczyk A, Svoboda K (2007): Channelrhodopsin-2-assisted circuit mapping of long-range callosal projections. Nat Neurosci 10:663–668.
51. Arenkiel BR, Peca J, Davison IG, Feliciano C, Deisseroth K, Augustine GJ, *et al.* (2007): In vivo light-induced activation of neural circuitry in transgenic mice expressing channelrhodopsin-2. Neuron 54:205–218.
52. Tye KM, Deisseroth K (2012): Optogenetic investigation of neural circuits underlying brain disease in animal models. Nat Rev Neurosci 13:251–256.
53. Lin JY, Knutsen PM, Muller A, Kleinfeld D, Tsien RY (2013): ReaChR: A red-shifted variant of channelrhodopsin enables deep transcranial optogenetic excitation. Nat Neurosci 16:1499–1508.
54. Klapoetke NC, Murata Y, Kim SS, Pulver SR, Birdsey-Benson A, Cho YK, *et al.* (2014): Independent optical excitation of distinct neural populations. Nat Methods 11:338–346.
55. Lin JY, Lin MZ, Steinbach P, Tsien RY (2009): Characterization of engineered channelrhodopsin variants with improved properties and kinetics. Biophys J 96:1803–1814.
56. Mattis J, Tye KM, Ferenczi EA, Ramakrishnan C, O'Shea DJ, Prakash R, *et al.* (2011): Principles for applying optogenetic tools derived from direct comparative analysis of microbial opsins. Nat Methods 9:159–172.
57. Fenno L, Yizhar O, Deisseroth K (2011): The development and application of optogenetics. Annu Rev Neurosci 34:389–412.
58. Han X, Qian X, Bernstein JG, Zhou HH, Franzesi GT, Stern P, *et al.* (2009): Millisecond-timescale optical control of neural dynamics in the nonhuman primate brain. Neuron 62:191–198.
59. Galvan A, Caiola MJ, Albaugh DL (2018): Advances in optogenetic and chemogenetic methods to study brain circuits in non-human primates. J Neural Transm (Vienna) 125:547–563.
60. Avermann M, Tomm C, Mateo C, Gerstner W, Petersen CC (2012): Microcircuits of excitatory and inhibitory neurons in layer 2/3 of mouse barrel cortex. J Neurophysiol 107:3116–3134.
61. Mao T, Kusefoglu D, Hooks Bryan M, Huber D, Petreanu L, Svoboda K (2011): Long-range neuronal circuits underlying the interaction between sensory and motor cortex. Neuron 72:111–123.
62. Hira R, Honkura N, Noguchi J, Maruyama Y, Augustine GJ, Kasai H, *et al.* (2009): Transcranial optogenetic stimulation for functional mapping of the motor cortex. J Neurosci Methods 179:258–263.
63. Ayling OG, Harrison TC, Boyd JD, Goroshkov A, Murphy TH (2009): Automated light-based mapping of motor cortex by photoactivation of channelrhodopsin-2 transgenic mice. Nat Methods 6:219–224.

64. Harrison TC, Silasi G, Boyd JD, Murphy TH (2013): Displacement of sensory maps and disorganization of motor cortex after targeted stroke in mice. Stroke 44:2300–2306.
65. Harrison TC, Ayling OG, Murphy TH (2012): Distinct cortical circuit mechanisms for complex forelimb movement and motor map topography. Neuron 74:397–409.
66. Sreenivasan V, Karmakar K, Rijli FM, Petersen CC (2014): Parallel pathways from motor and somatosensory cortex for controlling whisker movements in mice. Eur J Neurosci 41:354–367.
67. Lim DH, LeDue JM, Mohajerani MH, Murphy TH (2014): Optogenetic mapping after stroke reveals network-wide scaling of functional connections and heterogeneous recovery of the peri-infarct. J Neurosci 34:16455–16466.
68. Lim DH, Mohajerani MH, Ledue J, Boyd J, Chen S, Murphy TH (2012): In vivo large-scale cortical mapping using channelrhodopsin-2 stimulation in transgenic mice reveals asymmetric and reciprocal relationships between cortical areas. Front Neural Circuits 6:11.
69. Bovetti S, Moretti C, Zucca S, Dal Maschio M, Bonifazi P, Fellin T (2017): Simultaneous high-speed imaging and optogenetic inhibition in the intact mouse brain. Sci Rep 7:40041.
70. Akerboom J, Carreras Calderón N, Tian L, Wabnig S, Prigge M, Tolö J, *et al.* (2013): Genetically encoded calcium indicators for multi-color neural activity imaging and combination with optogenetics. Front Mol Neurosci 6:2.
71. Bauer AQ, Kraft AW, Baxter GA, Wright PW, Reisman MD, Bice AR, *et al.* (2018): Effective connectivity measured using optogenetically evoked hemodynamic signals exhibits topography distinct from resting state functional connectivity in the mouse. Cereb Cortex 28:370–386.
72. Desai M, Kahn I, Knoblich U, Bernstein J, Atallah H, Yang A, *et al.* (2011): Mapping brain networks in awake mice using combined optical neural control and fMRI. J Neurophysiol 105:1393–1405.
73. Lee JH, Durand R, Gradinaru V, Zhang F, Goshen I, Kim DS, *et al.* (2010): Global and local fMRI signals driven by neurons defined optogenetically by type and wiring. Nature 465:788–792.
74. Giorgi A, Migliarini S, Galbusera A, Maddaloni G, Mereu M, Margiani G, *et al.* (2017): Brain-wide mapping of endogenous serotonergic transmission via chemogenetic fMRI. Cell Reports 21: 910–918.
75. Grayson DS, Bliss-Moreau E, Machado CJ, Bennett J, Shen K, Grant KA, *et al.* (2016): The rhesus monkey connectome predicts disrupted functional networks resulting from pharmacogenetic inactivation of the amygdala. Neuron 91:453–466.
76. Roth BL (2016): DREADDs for neuroscientists. Neuron 89:683–694.
77. Kahn I, Desai M, Knoblich U, Bernstein J, Henninger M, Graybiel AM, *et al.* (2011): Characterization of the functional MRI response temporal linearity via optical control of neocortical pyramidal neurons. J Neurosci 31:15086–15091.
78. Anenberg E, Chan AW, Xie Y, LeDue JM, Murphy TH (2015): Optogenetic stimulation of GABA neurons can decrease local neuronal activity while increasing cortical blood flow. J Cereb Blood Flow Metab 35:1579–1586.
79. Scott NA, Murphy TH (2012): Hemodynamic responses evoked by neuronal stimulation via channelrhodopsin-2 can be independent of intracortical glutamatergic synaptic transmission. PLoS One 7:e29859.
80. Iordanova B, Vazquez AL, Poplawsky AJ, Fukuda M, Kim SG (2015): Neural and hemodynamic responses to optogenetic and sensory stimulation in the rat somatosensory cortex. J Cereb Blood Flow Metab 35:922–932.
81. Vazquez AL, Fukuda M, Crowley JC, Kim S-G (2014): Neural and hemodynamic responses elicited by forelimb- and photo-stimulation in channelrhodopsin-2 mice: Insights into the hemodynamic point spread function. Cereb Cortex 24:2908–2919.
82. Sirotin YB, Hillman EMC, Bordier C, Das A (2009): Spatiotemporal precision and hemodynamic mechanism of optical point spreads in alert primates. Proc Natl Acad Sci U S A 106:18390–18395.
83. Frostig RD, Lieke EE, Ts'o DY, Grinvald A (1990): Cortical functional architecture and local coupling between neuronal activity and the microcirculation revealed by in vivo high-resolution optical imaging of intrinsic signals. Proc Natl Acad Sci U S A 87:6082–6086.
84. Grinvald A, Lieke E, Frostig RD, Gilbert CD, Wiesel TN (1986): Functional architecture of cortex revealed by optical imaging of intrinsic signals. Nature 324:361–364.
85. Mohajerani MH, McVea DA, Fingas M, Murphy TH (2010): Mirrored bilateral slow-wave cortical activity within local circuits revealed by fast bihemispheric voltage-sensitive dye imaging in anesthetized and awake mice. J Neurosci 30:3745–3751.
86. Honey CJ, Sporns O, Cammoun L, Gigandet X, Thiran JP, Meuli R, *et al.* (2009): Predicting human resting-state functional connectivity from structural connectivity. Proc Natl Acad Sci U S A 106:2035–2040.
87. Poulet JFA, Fernandez LMJ, Crochet S, Petersen CCH (2012): Thalamic control of cortical states. Nat Neurosci 15:370–372.
88. Leong AT, Chan RW, Gao PP, Chan YS, Tsia KK, Yung WH, *et al.* (2016): Long-range projections coordinate distributed brain-wide neural activity with a specific spatiotemporal profile. Proc Natl Acad Sci U S A 113:E8306–E8315.
89. Chan RW, Leong ATL, Ho LC, Gao PP, Wong EC, Dong CM, *et al.* (2017): Low-frequency hippocampal-cortical activity drives brain-wide resting-state functional MRI connectivity. Proc Natl Acad Sci U S A 114:E6972–E6981.
90. Oh SW, Harris JA, Ng L, Winslow B, Cain N, Mihalas S, *et al.* (2014): A mesoscale connectome of the mouse brain. Nature 508:207–214.
91. Ferezou I, Haiss F, Gentet LJ, Aronoff R, Weber B, Petersen CCH (2007): Spatiotemporal dynamics of cortical sensorimotor integration in behaving mice. Neuron 56:907–923.
92. Matsui T, Tamura K, Koyano KW, Takeuchi D, Adachi Y, Osada T, *et al.* (2011): Direct comparison of spontaneous functional connectivity and effective connectivity measured by intracortical microstimulation: An fMRI study in macaque monkeys. Cereb Cortex 21:2348–2356.
93. Buzsáki G, Moser EI (2013): Memory, navigation and theta rhythm in the hippocampal-entorhinal system. Nat Neurosci 16:130–138.
94. Hahn TT, Sakmann B, Mehta MR (2007): Differential responses of hippocampal subfields to cortical up-down states. Proc Natl Acad Sci U S A 104:5169–5174.
95. Sherman SM, Guillery RW (1996): Functional organization of thalamocortical relays. J Neurophysiol 76:1367–1395.
96. Schiff Nicholas D (2008): Central thalamic contributions to arousal regulation and neurological disorders of consciousness. Ann N Y Acad Sci 1129:105–118.
97. Liu J, Lee HJ, Weitz AJ, Fang Z, Lin P, Choy M, *et al.* (2015): Frequency-selective control of cortical and subcortical networks by central thalamus. Elife 4:e09215.
98. Weitz AJ, Fang Z, Lee HJ, Fisher RS, Smith WC, Choy M, *et al.* (2015): Optogenetic fMRI reveals distinct, frequency-dependent networks recruited by dorsal and intermediate hippocampus stimulations. Neuroimage 107:229–241.
99. Barker AT, Jalinous R, Freeston IL (1985): Non-invasive magnetic stimulation of human motor cortex. Lancet 1:1106–1107.
100. Hallett M (2007): Transcranial magnetic stimulation: A primer. Neuron 55:187–199.
101. Hoogendam JM, Ramakers GM, Di Lazzaro V (2010): Physiology of repetitive transcranial magnetic stimulation of the human brain. Brain Stimul 3:95–118.
102. Huang YZ, Edwards MJ, Rounis E, Bhatia KP, Rothwell JC (2005): Theta burst stimulation of the human motor cortex. Neuron 45: 201–206.
103. Allen EA, Pasley BN, Duong T, Freeman RD (2007): Transcranial magnetic stimulation elicits coupled neural and hemodynamic consequences. Science 317:1918–1921.
104. Valero-Cabre A, Payne BR, Rushmore J, Lomber SG, Pascual-Leone A (2005): Impact of repetitive transcranial magnetic stimulation of the parietal cortex on metabolic brain activity: A 14C-2DG tracing study in the cat. Exp Brain Res 163:1–12.
105. Salinas FS, Szabo CA, Zhang W, Jones L, Leland MM, Wey HY, *et al.* (2011): Functional neuroimaging of the baboon during concurrent

image-guided transcranial magnetic stimulation. Neuroimage 57:1393–1401.
106. Gratton C, Lee TG, Nomura EM, D'Esposito M (2014): Perfusion MRI indexes variability in the functional brain effects of theta-burst transcranial magnetic stimulation. PLoS One 9:e101430.
107. Chiang TC, Vaithianathan T, Leung T, Lavidor M, Walsh V, Delpy DT (2007): Elevated haemoglobin levels in the motor cortex following 1 Hz transcranial magnetic stimulation: A preliminary study. Exp Brain Res 181:555–560.
108. Pasley BN, Allen EA, Freeman RD (2009): State-dependent variability of neuronal responses to transcranial magnetic stimulation of the visual cortex. Neuron 62:291–303.
109. Ruff CC, Driver J, Bestmann S (2009): Combining TMS and fMRI: From 'virtual lesions' to functional-network accounts of cognition. Cortex 45:1043–1049.
110. Rahnev D, Kok P, Munneke M, Bahdo L, de Lange FP, Lau H (2013): Continuous theta burst transcranial magnetic stimulation reduces resting state connectivity between visual areas. J Neurophysiol 110:1811–1821.
111. Cohen LG, Celnik P, Pascual-Leone A, Corwell B, Falz L, Dambrosia J, *et al.* (1997): Functional relevance of cross-modal plasticity in blind humans. Nature 389:180–183.
112. Lowe CJ, Manocchio F, Safati AB, Hall PA (2018): The effects of theta burst stimulation (TBS) targeting the prefrontal cortex on executive functioning: A systematic review and meta-analysis. Neuropsychologia 111:344–359.
113. Wang JX, Rogers LM, Gross EZ, Ryals AJ, Dokucu ME, Brandstatt KL, *et al.* (2014): Targeted enhancement of cortical-hippocampal brain networks and associative memory. Science 345:1054–1057.
114. Bodart O, Amico E, Gomez F, Casali AG, Wannez S, Heine L, *et al.* (2018): Global structural integrity and effective connectivity in patients with disorders of consciousness. Brain Stimul 11:358–365.
115. Marshall TR, O'Shea J, Jensen O, Bergmann TO (2015): Frontal eye fields control attentional modulation of alpha and gamma oscillations in contralateral occipitoparietal cortex. J Neurosci 35:1638–1647.
116. Siebner HR, Bergmann TO, Bestmann S, Massimini M, Johansen-Berg H, Mochizuki H, *et al.* (2009): Consensus paper: Combining transcranial stimulation with neuroimaging. Brain Stimul 2:58–80.
117. Groiss SJ, Mochizuki H, Furubayashi T, Kobayashi S, Nakatani-Enomoto S, Nakamura K, *et al.* (2013): Quadri-pulse stimulation induces stimulation frequency dependent cortical hemoglobin concentration changes within the ipsilateral motor cortical network. Brain Stimul 6:40–48.
118. Ruff CC, Blankenburg F, Bjoertomt O, Bestmann S, Freeman E, Haynes JD, *et al.* (2006): Concurrent TMS-fMRI and psychophysics reveal frontal influences on human retinotopic visual cortex. Curr Biol 16:1479–1488.
119. Bergmann TO, Karabanov A, Hartwigsen G, Thielscher A, Siebner HR (2016): Combining non-invasive transcranial brain stimulation with neuroimaging and electrophysiology: Current approaches and future perspectives. Neuroimage 140:4–19.
120. Massimini M, Ferrarelli F, Sarasso S, Tononi G (2012): Cortical mechanisms of loss of consciousness: Insight from TMS/EEG studies. Arch Ital Biol 150:44–55.
121. Reithler J, Peters JC, Sack AT (2011): Multimodal transcranial magnetic stimulation: Using concurrent neuroimaging to reveal the neural network dynamics of noninvasive brain stimulation. Prog Neurobiol 94:149–165.
122. Driver J, Blankenburg F, Bestmann S, Vanduffel W, Ruff CC (2009): Concurrent brain-stimulation and neuroimaging for studies of cognition. Trends Cogn Sci 13:319–327.
123. Blankenburg F, Ruff CC, Bestmann S, Bjoertomt O, Eshel N, Josephs O, *et al.* (2008): Interhemispheric effect of parietal TMS on somatosensory response confirmed directly with concurrent TMS-fMRI. J Neurosci 28:13202–13208.
124. Bestmann S, Swayne O, Blankenburg F, Ruff CC, Haggard P, Weiskopf N, *et al.* (2008): Dorsal premotor cortex exerts state-dependent causal influences on activity in contralateral primary motor and dorsal premotor cortex. Cereb Cortex 18:1281–1291.
125. Fox MD, Buckner RL, Liu H, Chakravarty MM, Lozano AM, Pascual-Leone A (2014): Resting-state networks link invasive and noninvasive brain stimulation across diverse psychiatric and neurological diseases. Proc Natl Acad Sci U S A 111:E4367–E4375.
126. Nowak DA, Bosl K, Podubecka J, Carey JR (2010): Noninvasive brain stimulation and motor recovery after stroke. Restor Neurol Neurosci 28:531–544.
127. de Hemptinne C, Swann NC, Ostrem JL, Ryapolova-Webb ES, San Luciano M, Galifianakis NB, *et al.* (2015): Therapeutic deep brain stimulation reduces cortical phase-amplitude coupling in Parkinson's disease. Nat Neurosci 18:779–786.
128. Lefaucheur JP (2009): Treatment of Parkinson's disease by cortical stimulation. Expert Rev Neurother 9:1755–1771.
129. Philip NS, Barredo J, Aiken E, Carpenter LL (2018): Neuroimaging mechanisms of therapeutic transcranial magnetic stimulation for major depressive disorder. Biol Psychiatry Cogn Neurosci Neuroimaging 3:211–222.
130. Fox MD, Buckner RL, White MP, Greicius MD, Pascual-Leone A (2012): Efficacy of transcranial magnetic stimulation targets for depression is related to intrinsic functional connectivity with the subgenual cingulate. Biol Psychiatry 72:595–603.
131. Weigand A, Horn A, Caballero R, Cooke D, Stern AP, Taylor SF, *et al.* (2018): Prospective validation that subgenual connectivity predicts antidepressant efficacy of transcranial magnetic stimulation sites. Biol Psychiatry 84:28–37.
132. Heller AS (2016): Cortical-subcortical interactions in depression: From animal models to human psychopathology. Front Syst Neurosci 10:20.
133. Covington HE 3rd, Lobo MK, Maze I, Vialou V, Hyman JM, Zaman S, *et al.* (2010): Antidepressant effect of optogenetic stimulation of the medial prefrontal cortex. J Neurosci 30:16082–16090.
134. Nestler EJ, Carlezon WA Jr (2006): The mesolimbic dopamine reward circuit in depression. Biol Psychiatry 59:1151–1159.
135. Bjorklund A, Dunnett SB (2007): Dopamine neuron systems in the brain: An update. Trends Neurosci 30:194–202.
136. Lohani S, Poplawsky AJ, Kim SG, Moghaddam B (2016): Unexpected global impact of VTA dopamine neuron activation as measured by opto-fMRI. Mol Psychiatry 22:585.
137. Mitra A, Kraft A, Wright P, Acland B, Snyder AZ, Rosenthal Z, *et al.* (2018): Spontaneous infra-slow brain activity has unique spatiotemporal dynamics and laminar structure. Neuron 98: 297–305.e6.
138. Wright PW, Brier LM, Bauer AQ, Baxter GA, Kraft AW, Reisman MD, *et al.* (2017): Functional connectivity structure of cortical calcium dynamics in anesthetized and awake mice. PLoS One 12:e0185759.
139. Schlegel F, Sych Y, Schroeter A, Stobart J, Weber B, Helmchen F, *et al.* (2018): Fiber-optic implant for simultaneous fluorescence-based calcium recordings and BOLD fMRI in mice. Nat Protoc 13:840.
140. Ma Y, Shaik MA, Kozberg MG, Kim SH, Portes JP, Timerman D, *et al.* (2016): Resting-state hemodynamics are spatiotemporally coupled to synchronized and symmetric neural activity in excitatory neurons. Proc Natl Acad Sci U S A 113:E8463–E8471.
141. Srinivasan R, Lu T-Y, Chai H, Xu J, Huang BS, Golshani P, *et al.* (2016): New transgenic mouse lines for selectively targeting astrocytes and studying calcium signals in astrocyte processes in situ and in vivo. Neuron 92:1181–1195.
142. Platisa J, Pieribone VA (2018): Genetically encoded fluorescent voltage indicators: Are we there yet? Curr Opin Neurobiol 50: 146–153.
143. Chen TW, Wardill TJ, Sun Y, Pulver SR, Renninger SL, Baohan A, *et al.* (2013): Ultrasensitive fluorescent proteins for imaging neuronal activity. Nature 499:295–300.
144. Adam Y, Kim JJ, Lou S, Zhao Y, Brinks D, Wu H, *et al.* (2018): All-optical electrophysiology reveals brain-state dependent changes in

hippocampal subthreshold dynamics and excitability [published online ahead of print Mar 13]. bioRxiv.

145. Marshall JD, Li JZ, Zhang Y, Gong Y, St-Pierre F, Lin MZ, *et al.* (2016): Cell-type-specific optical recording of membrane voltage dynamics in freely moving mice. Cell 167:1650–1662.e15.

146. John M. Eisenberg Center for Clinical Decisions and Communications Science (2011): Nonpharmacologic Interventions for Treatment-Resistant Depression in Adults. Rockville, MD: Agency for Healthcare Research and Quality.

147. Razza LB, Moffa AH, Moreno ML, Carvalho AF, Padberg F, Fregni F, *et al.* (2018): A systematic review and meta-analysis on placebo response to repetitive transcranial magnetic stimulation for depression trials. Prog Neuropsychopharmacol Biol Psychiatry 81:105–113.

148. Schaeffer DJ, Johnston KD, Gilbert KM, Gati JS, Menon RS, Everling S (2018): In vivo manganese tract tracing of frontal eye fields in rhesus macaques with ultra-high field MRI: Comparison with DWI tractography. Neuroimage 181:211–218.